THE JOURNAL OF PHYSICAL CHEMISTRY C

Article

pubs.acs.org/JPCC

Thermal Conductance across Phosphonic Acid Molecules and Interfaces: Ballistic versus Diffusive Vibrational Transport in Molecular Monolayers

John T. Gaskins,[†] Anuradha Bulusu,[‡] Anthony J. Giordano,[§] John C. Duda,[†] Samuel Graham,*[,‡] and Patrick E. Hopkins*[,†]

[†]Department of Mechanical and Aerospace Engineering, University of Virginia, Charlottesville, Virginia 22904, United States

[‡]Woodruff School of Mechanical Engineering and [§]School of Chemistry and Biochemistry, Georgia Institute of Technology, Atlanta, Georgia 30332, United States

Supporting Information

ABSTRACT: The influence of planar organic linkers on thermal boundary conductance across hybrid interfaces has focused on the organic/inorganic interaction energy rather than on vibrational mechanisms in the molecule. As a result, research into interfacial transport at planar organic monolayer junctions has treated molecular systems as thermally ballistic. We show that thermal conductance in phosphonic acid (PA) molecules is ballistic, and the thermal boundary conductance across metal/PA/sapphire interfaces is driven by the same phononic processes as those across metal/sapphire interfaces without PAs, with one exception. We find a more than 40% reduction in conductance across henicosafluorododecylphosphonic acid (F21PA) interfaces, independent of metal contact, despite similarities in structure, composition, and terminal group to the variety of other PAs studied. Our results suggest diffusive scattering of thermal vibrations in F21PA, demonstrating a clear path toward modification of interfacial thermal transport based on knowledge of ballistic and diffusive scattering in single monolayer molecular interfacial films.

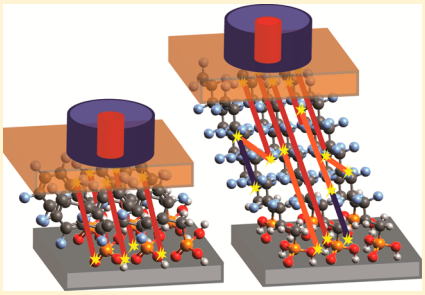

INTRODUCTION

The ability to precisely control the transfer of heat in nanostructures would provide novel thermal solutions for a wide variety of applications but heretofore has been difficult to achieve. As the magnitude of carrier mean free paths approach or exceed intrinsic length scales of relevant material systems, the majority of thermal carrier interactions are dictated by material boundaries and interfaces. This has led to exciting new realizations in thermal transport in nanosystems, including coherent phonon transport in superlattices,[1,2] electron "tunneling" through materials in multilayers,[3] crystalline materials with thermal conductivities lower than their corresponding amorphous phases,[4−6] and competing long- and short-wavelength phonon scattering mechanisms leading to size effects in alloy films and superlattices.[7,8] Despite these significant advances, further progress toward discovering, understanding, and utilizing these unique nanoscale thermal transport processes would be greatly facilitated by the ability to manipulate interactions at boundaries and interfaces with atomic or molecular resolution.

The thermal transport across interfaces between two solids, which is often characterized by the thermal boundary conductance[9] or Kapitza conductance[10] (h_K), can be difficult to predict and control since h_K is related to properties of the interface as well as the fundamental properties of the materials comprising the interface. Recent advances in manipulating the thermal boundary conductance across solid interfaces have relied on disrupting the local atomic order and/or structure around solid/solid interfaces (for a recent review, see ref 11). For example, changes in thermal conductance across solid boundaries have been experimentally observed by considering geometric roughness,[12−14] chemical mixing,[10,15,16] crystalline orientation,[17,18] strain,[19] and defects.[20−22] Where these structural modifications to the interfaces often rely on some disorder driven by the atomic arrangement, several recent measurements have confirmed an additional, if not more effective, avenue to tune the thermal boundary conductance between two solids driven by the chemical bond at the interface.[23−27] With the availability of a wide array of molecules and functional groups, new materials and composite interfaces that utilize interfacial chemistries and bonding have provided a pathway to alter thermal transport at the molecular level, including functionalized fullerene derivatives that set new extremes to the lowest thermal conductivity for a fully dense solid,[28−30] organic and/or inorganic crystalline multilayers with glass-like thermal conductivities,[31,32] and functionalized nanocrystalline arrays with nanoparticle-size-tunable thermal transport.[33,34]

Received: June 8, 2015
Revised: August 5, 2015
Published: August 17, 2015

DOI: 10.1021/acs.jpcc.5b05462
J. Phys. Chem. C 2015, 119, 20931−20939

These aforementioned examples highlight the potential for the use of molecular interfaces to pave a new path forward for tailoring thermal transport in nanosystems. Previous research has focused on theoretical and computational modeling of heat transport in self-assembled monolayers (SAMs) and across low-dimensional molecular interfaces.[25,35−37] However, experimental data on measuring and understanding the fundamental vibrational scattering processes driving thermal conducatance at planar, solid-based molecular functionalized single interfaces have been restricted to SAMs of alkanes.[38−45] Additionally, there have been a number of studies assessing the effects of molecular interfaces on solid−liquid thermal boundary conductance and vibrational energy transport using a variety of SAM layers.[46−49] Recent works using phosphonic acid (PA) molecules have demonstrated the ability of 12-mercapto-dodecylphosphonic acid (MDPA) to strengthen the bond between Au and TiO_2, leading to an increase in h_K.[24,26] This result focusing on PA molecules suggests a new class of molecular interfaces may be used to atomistically manipulate interfacial transport. Unfortunately, the understanding of PA interfacial thermal transport is currently limited to Au/MDPA/TiO_2 interfaces, and thus a void exists in the physics of heat transfer in systems composed of PA's.

As the current state of the literature is restricted to one particular class of PA interface, questions still remain about how PAs can be used to manipulate the thermal conductance across boundaries. For example, it is often assumed that thermal vibrations will not interact anharmonically within a SAM and the majority of the vibrational scattering occurs at the SAM boundaries. However, where this assumption has been rigorously studied both computationally and experimentally for alkanes,[35−39,41,50] the validity of this assumption for PAs has not been addressed. Given the diversity of the functional tail groups available for PA SAMs, PAs may provide a useful platform to study how vibrational energy travels through a molecule and across the bond it forms with surfaces. Ong et al. studied thermal transport in PA-based nanocrystalline arrays, utilizing pump−probe metrologies similar to those used in this work, and demonstrated that heat transport across solid/molecular interfaces is driven by interactions of vibrations of similar energies (i.e., elastic scattering events). O'Brien et al. and Chow et al. performed experimental measurements across Au/MDPA/TiO_2 interfaces[24,26] using time-domain thermoreflectance (TDTR), the same technique used here, and concluded that thermal transport is governed by the high interfacial bond strength characteristic of MDPA interfaces. Previous research in our group has shown both computationally[51] and experimentally[23] that an increase in bond strength leads to an increase in h_K due to inelastic scattering events (e.g., phonon conversion to different energies across the interface).[52] Unfortunately, the reported experimental results on Au/MDPA/TiO_2[24,26] do not lend insight into how vibrational heat is transported across solid/molecular interfaces. As a result, the limited data on PA-based interfaces do not provide the necessary thermophysics to validate PA-based molecular interfaces as thermally engineered materials. Given the widespread use of PA molecular interfaces in organic electronics,[53−56] improved understanding of how heat is transferred across PA modified interfaces is of great interest to a wide array of scientific communities.

Phosphonic acids consist of a polar headgroup consisting of the phosphoryl bond (P═O) and two P−O−H bonds, in addition to a linker or chain group followed by a functional tail group (R) as shown in Figure 1. The length of the chain can vary depending on the molecule: a long chain of 2 nm

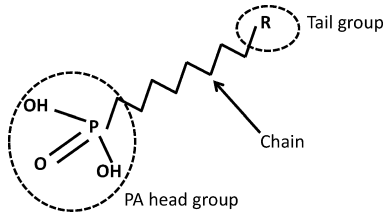

Figure 1. Structure of a phosphonic acid molecule.

corresponding to F21PA ((3,3,4,4,5,5,6,6,7,7,8,8,9,9,10,-10,11,11,12,12,12-henicosafluorododecyl)phosphonic acid), 1.3 nm for octylphosphonic acid (OPA), and a short chain less than 1 nm for PFBPA (pentafluorobenzylphosphonic acid).[57,58] The composition of the chain and its length affect the thickness and orientation of the molecule in the monolayer in addition to acting as a barrier between the head and tail groups. The nature of the terminal functional group, also known as the tail group, determines the overall surface energy and chemical attributes of the PA-modified substrate.[53,54,59] The binding of phosphonic acids to various substrates has been widely investigated and has been determined to be dependent on the nature of the metallic oxide substrate where the acids generally tend to covalently bond with the surface as a M−O−P bond in either a mono-, bi-, or tridentate fashion leading to hydrolytically stable bonds.[53,55,56,60−64]

In order to fully elucidate how vibrational energy is transmitted through PA-modified interfaces, we conduct an extensive study of the thermal conductance across metal/PA/single crystalline sapphire interfaces. We choose sapphire as our substrate for this study for several reasons: (i) PAs have been shown to form strong and highly stable covalent bonds on metal oxide surfaces;[54,65] in particular, PA modification of single crystalline and native oxide alumina substrates for adhesion promotion and corrosion inhibition has long been explored in great detail and found to be a safe and hydrolytically stable alternative to traditionally used metal ion inhibitors.[62,66] This strong, chemisorbed PA/sapphire bond allows us to evaluate how the metal/PA bond and scattering in the PA affect conductance: (ii) single crystalline sapphire has a relatively high thermal conductivity which results in a high sensitivity to the thermal conductance across the metal/PA/sapphire interface,[67] and (iii) the thermal boundary conductance across metal/sapphire interfaces (without PA surface modifications) has been extensively studied in previous literature providing sufficient data and physical understanding for broad interpretation of our results.[17,68−73]

We prepare different types of interfaces with different metal/PA combinations on *c*-plane sapphire and measure the thermal boundary conductance with time-domain thermoreflectance (TDTR).[67,74,75] Our measurements show that the thermal boundary conductance across a wide array of metal/PA/sapphire interfaces are driven by the same processes that dictate heat transfer across metal/sapphire interfaces without the PA molecule; this finding is consistent with recent work by Majumdar, where it was demonstrated that the vibrational mismatch of the metal contacts controls the thermal conductance across metal/self-assembled monolayer/metal interfaces.[76] Furthermore, we find a large reduction in conductance across the metal/F21PA/sapphire interfaces.

DOI: 10.1021/acs.jpcc.5b05462
J. Phys. Chem. C 2015, 119, 20931−20939

Table 1. Details of the Various Phosphonic Acids Used in This Study

phosphonic acid	chain length (nm)	molecular formula	polarity of tail group	mol wt (g/mol)
phenylphosphonic acid (PPA)	~0.9	$C_6H_7O_3P$	nonpolar[60]	158.09
2,3,4,5,6-pentafluorobenzylphosphonic acid (PFBPA)	~0.9	$C_7H_4F_5O_3P$	nonpolar[53]	262.07
octylphosphonic acid (OPA)	~1.3	$C_8H_{19}O_3P$	nonpolar[81,82]	194.21
11-hydroxyundecylphosphonic acid (HUPA)	~1.5	$C_{11}H_{25}O_4P$	polar	252.29
(3,3,4,4,5,5,6,6,7,7,8,8,8-tridecafluorooctyl)phosphonic acid (FHOPA)	~1.2	$C_8H_6F_{13}O_3P$	nonpolar[53]	428.08
(3,3,4,4,5,5,6,6,7,7,8,8,9,9,10,10,11,11,12,12,12-henicosafluorododecyl)phosphonic acid (F21PA)	~2	$C_{12}H_6F_{21}O_3P$	nonpolar[77]	628.11

Henicosafluorododecylphosphonic acid (F21PA) is known for its extremely high nonpolarity due to the presence of 21 fluorine atoms in its chain and tail as evidenced from its extremely high water contact angle of 121° on AlO_x surfaces;[77] F21PA is also a large molecule with a molecular weight greater than the other PA investigated in this study. Given the similar head and tail functionalities of all the PAs that we investigate, we conclude that the reduction in h_K across the F21PA interfaces is due to diffusive scattering of thermal vibrations in the F21PA molecule; we note that this behavior has not been observed in any previous literature focused on the thermal conductance of alkanes.[35−39,41] The temperature trends of the thermal conductance per unit area of the F21PA molecule suggest that thermal vibrations are interacting anharmonically in the molecule, consistent with previous analyses of the thermal conductivity trends in amorphous materials with complex unit cells, polymers, and solid proteins.[78−80] To the best of our knowledge, this is the first observation of diffusive scattering of thermal vibrations in an interface-modifying molecule.

RESULTS AND DISCUSSION

We studied various metal/PA/sapphire interfacial combinations with three different types of metals aluminum (Al), nickel (Ni), and gold (Au) and five phosphonic acids as listed in Table 1. The structures of the various phosphonic acids are shown in Figure 2. The choice of acids was based on two criteria: (1) chain length and (2) polarity of the tail group. Chain length and polarity of the tail groups reported in Table 1 were taken from a variety of reported values in the literature.[53,60,77,81,82] The phenylphosphonic acid (PPA, CAS # 1571-33-1) and octylphosphonic acid (OPA, CAS # 4724-48-5) molecules were obtained from Sigma-Aldrich while the 11-hydroxyundecylphosphonic acid (HUPA, CAS # 83905-98-0) was obtained from Sikemia. The 2,3,4,5,6-pentafluorobenzylphosphonic acid (PFBPA, CAS # 137174-84-6), 1*H*,1*H*,2*H*,2*H*-perfluoro-*n*-octylphosphonic acid (FHOPA) and 3,3,4,4,5,5,6,6,7,7,8,8,9,-9,10,10,11,11,12,12,12-henicosafluorododecylphosphonic acid (F21PA, CAS # 252237-39-1) were synthesized as previously described and described in detail in the Supporting Information.[53,77]

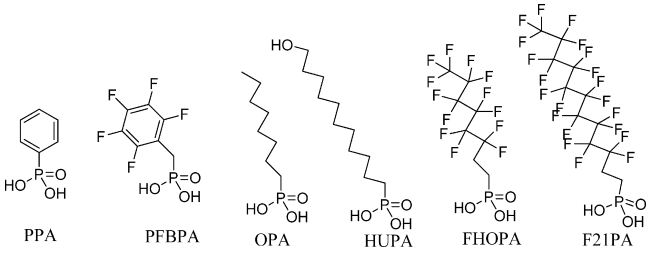

Figure 2. Molecular structure of the various phosphonic acids used in this study.

The thermal boundary conductance, h_K, between the various metal/PA/sapphire interfaces was measured with time-domain thermoreflectance (TDTR). The technique is described thoroughly elsewhere,[67,74,75,83] and our specific experimental details, including a discussion of error and sensitivity of TDTR to measuring thermal boundary conductance, are outlined in the Supporting Information. Table 2 summarizes the room temperature results of thermal boundary conductance measurements on the different metal/PA/sapphire combinations, which are plotted in Figure 3 as a function of PA molecular weight to interrogate the effects of molecular size on the measured conductance across the molecule and associated interfaces. Examining Figure 3, it is clear that the addition of a molecule between the metal and sapphire has little effect on the thermal boundary conductance for the majority of the PA modified interfaces. However, in the case of the heaviest molecule investigated in this study, F21PA, a decrease is seen regardless of choice of metallic transducer. It is unlikely this reduction in thermal boundary conduction is due to the bonding between

Table 2. Sample Details of the Various Metal/PA/Sapphire Interfaces, Molecular Weights, Terminating Groups Chemistry at the Metal/PA Interface, and Thermal Boundary Conductances across the Metal/PA/Sapphire Interfaces at Room Temperature

metal	phosphonic acid[a]	mol wt (g mol^{-1})	metal/PA chemistry	h_K (MW m^{-2} K^{-1})
Al	none			164.4 ± 15.8
	PFBPA	262.1	(C_6F_5)	169.3 ± 13.0
	OPA	194.2	C_8H_{17}	142.5 ± 12.5
	PPA	158.1	(C_6H_5)	184.8 ± 16.5
	FHOPA	428.08	C_6F_{13}	140.6 ± 14.2
	F21PA	628.1	$C_{10}F_{21}$	60.3 ± 4.5
Au	none			74.3 ± 8.6
	F21PA	628.1	$C_{10}F_{21}$	45.8 ± 6.4
Ni	none			197.4 ± 20.0
	PFBPA	262.1	(C_6F_5)	181.6 ± 18.2
	OPA	194.2	C_8H_{17}	188.4 ± 25.5
	HUPA	252.3	$C_{11}H_{24}$-OH	214.2 ± 21.2
	FHOPA	428.08	C_6F_{13}	213.5 ± 25.7
	F21PA	628.1	$C_{10}F_{21}$	65.3 ± 6.1

[a]2,3,4,5,6-Pentafluorobenzylphosphonic acid (PFBPA), octylphosphonic acid (OPA), phenylphosphonic acid (PPA), 3,3,4,4,5,5,6,6,7,7,8,8,8-tridecafluorooctylphosphonic acid (FHOPA), 3,3,4,4,5,5,6,6,7,7,8,8,9,9,10,10,11,11,12,12,12-henicosafluorododecylphosphonic acid (F21PA), and 11-hydroxyundecylphosphonic acid (HUPA).

DOI: 10.1021/acs.jpcc.5b05462
J. Phys. Chem. C 2015, 119, 20931−20939

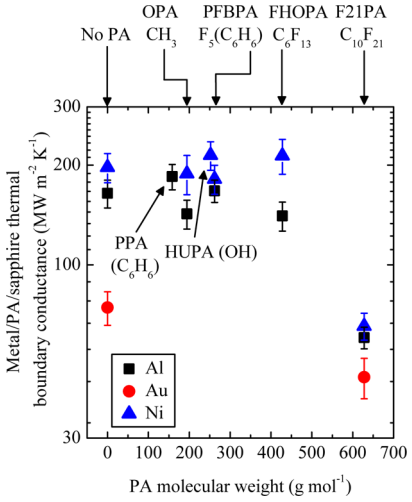

Figure 3. Thermal boundary conductance as a function of molecular weight for the various metal/PA/sapphire interfaces measured in this work. Within the uncertainty in our measurements, we do not observe any appreciable change in the thermal boundary conductance across the Al/PA or Ni/PA interfaces for the PPA, OPA, PFBPA, FHOPA, and HUPA interface. However, F21PA, which is a large molecule, leads to a reduction in the thermal boundary conductance across all metal/sapphire interfaces.

the metal and the fluorine termination of the tail group in F21PA, as similarly terminated PAs, FHOPA and PFBPA, exhibit no change in thermal boundary conductance from the control sample. Additionally, the length of F21PA (~2 nm) is likely not the source of the large reduction in conductance as HUPA (~1.7 nm) has a similar length and also does not show a reduction in conductance compared to the control.

The relatively larger reduction in boundary conductance for both the Ni- and Al-capped films, compared with the gold transducer, is likely due to the differences in Debye temperature (Ni 450 K, Al 428 K, Au 165 K) of the metals,[84] which governs the available vibrational modes able to transfer across the interface into the sapphire substrate.[85] Our previous work showed that the temperature derivative of the phonon flux from the metal is the major contribution to changes in thermal boundary conductance when comparing different metal/nonmetal interfaces, including metal/sapphire combinations.[85] For control samples without PAs between the metal and sapphire, the thermal boundary conductances are consistent with this analysis where larger phonon spectra and velocities result in a larger thermal boundary conductance. The fixed resistance added to this interface from the F21PA molecule causes a large reduction in conductance across the Al and Ni interfaces due to the intrinsically high conductance of this interface originating from the high phonon flux in the metals. The Au/sapphire interface conductance is intrinsically lower than the Al and Ni, so the resistance added from the F21PA molecule does not have as significant of an impact on the heat flow across these Au-metallized interfaces as compared to the Al- and Ni-based interfaces. We attribute this reduction in thermal boundary conductance with the inclusion of the F21PA molecule to a reduction in phonon transmission across the PA molecule, as we discuss in more detail with respect to all of the PA interfaces below.

We measure the thermal boundary conductance across various metal/PA/sapphire interfaces over a range of temperatures to investigate the trends in vibrational transport and corresponding interfacial transmission. Figure 4 shows measurements of aluminum/PA/sapphire samples of different

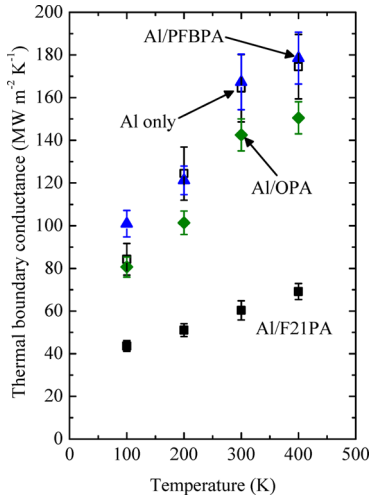

Figure 4. Thermal boundary conductance as a function for temperature for various Al/PA/sapphire interfaces. We do not observe any appreciable difference between the Al/sapphire, Al/OPA/sapphire, and Al/PFBPA/sapphire thermal boundary conductance within the uncertainty of our TDTR measurement. The similar temperature dependency in h_K among these interfaces suggests that these PAs transport energy ballistically and the thermal boundary conductance across the PA interfaces is elastic and extremely high relative to the Al/sapphire interface. Conversely, a large reduction in h_K is observed at the Al/F21PA/sapphire interface compared to the other interfaces. We attribute this to diffusive vibrational scattering in the F21PA SAM.

PA molecular weights over a temperature range from 100 to 400 K. The lighter molecules, relative to the weight of F21PA, exhibit similar trends in both magnitude and curvature. Given the negligible modification to thermal boundary conductance across PFBPA and OPA compared to the unmodified interface, we conclude that heat transport across these PA contacts is driven by the phononic spectra in the metal and sapphire and not influenced by the vibrational spectra of the PAs. This is consistent with Majumdar's findings, providing further evidence that conductance through the non-F21PA phosphonic acid molecules is ballistic.[76] It is important to note that PFBPA terminates in fluorine, similar to F21PA, and as such we believe that the difference in trends between these molecules is not due to interfacial bonding effects. Furthermore, these results imply that the phonon transmission across the metal/PA and PA/sapphire interfaces are relatively high, much higher than the intrinsic transmission across the metal/sapphire interface, and as such do not affect the overall transmission of the phonon flux from the metal to sapphire.

Insight into the reduction in thermal boundary conductance for the Al/F21PA/sapphire molecule is garnered by qualitatively examining the temperature trends in Figure 4. The slope of the conductance across Al/F21PA/sapphire interface as a function of temperature is shallower than the control or the samples with less massive molecules. Having previously ruled out both Al/PA and PA/sapphire contact effects as appreciable resistances, we attribute this to diffusive vibrational scattering in the F21PA molecule. This diffusive scattering adds a temperature-dependent resistance to the overall Al/F21PA/sapphire thermal transport, indicated by the change magnitude and slope

DOI: 10.1021/acs.jpcc.5b05462
J. Phys. Chem. C 2015, 119, 20931−20939

of the temperature trends measured in the thermal boundary conductance. This is in stark contrast to the PFBPA and OPA interfaces where the similar temperature trends in h_K, which are comparable to the Al/sapphire control, suggest ballistic transport of heat is the characteristic energy transmission mechanism through these molecules.

To highlight the role of the metal/PA interface in our analysis and test our hypothesis of diffusive scattering in the F21PA molecule, we compare the measured thermal boundary conductance across Al/F21PA/sapphire and Au/F21PA/sapphire interfaces as a function of temperature in Figure 5.

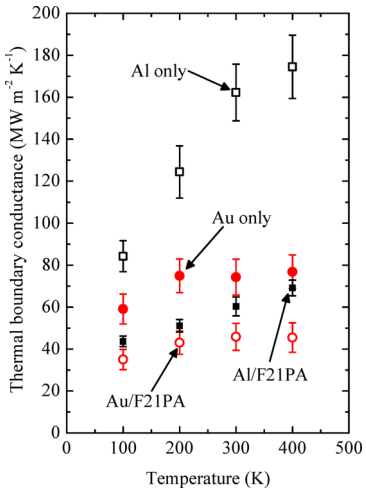

Figure 5. Effect of F21PA on the thermal boundary conductance across Al/sapphire and Au/sapphire interfaces is noticeable via a comparison of the thermal boundary conductance across each interface. At both metal interfaces, F21PA causes an appreciable reduction in the thermal boundary conductance due to diffusive scattering in the F21PA molecule.

Even for the low conductance Au/sapphire interface, an appreciable reduction in the thermal boundary conductance across the Au/F21PA/sapphire interface is observed. The addition of the F21PA molecule modifies the slope in conductance vs temperature across the Al/sapphire interface, and the inclusion of F21PA causes a shift in the conductance values without any appreciable change in the temperature trends for the Au-coated samples. This is consistent with our previous discussion regarding the available phonon modes and thermal flux in the metal driving thermal conductance. For the Au film, the vibrational states in the Au are fully (or nearly fully) populated as the measurement temperatures approach or exceed gold's Debye temperature of 165 K. Therefore, given that the phonon flux in Au limits the conductance, this further supports our conclusion that phonon transmission across the Au/F21PA contact is dominated by elastic scattering of vibrations with similar energies. The role of the F21PA is to add resistance to the interface but not to facilitate in any mode conversion during transmission of vibrations from the Au, through the F21PA, and into the sapphire. This also suggests the reduction in magnitude of h_K being due to diffusive vibrational scattering in the F21PA molecule, as this interfacial structure reduces the probability of phonons transmitting from the metal to the sapphire. This is also consistent with the temperature trends observed in the Al-coated samples in Figure 5. The fact that the increase in h_K with temperature is less pronounced and that h_K is lower with the addition of the F21PA molecule points to a reduction in elastic phonon transmission across the Al/F21PA/sapphire interface as compared to the Al/sapphire interface. This is consistent with our previous analyses of thermal boundary conductance across Al/silicon interfaces with and without a native oxide and varying degrees of interfacial roughness and disorder.[12−14,21]

Given our conclusion regarding the elastic vibrational coupling across the metal/F21PA and F21PA/sapphire interfaces, we can treat the resistance of the F21PA molecule as a resistor in series with the metal/sapphire resistance; note, this approach is consistent with previous analyses of the native oxide layer between aluminum and silicon[13,14,21] and an Al_2O_3 layer between Al and Si or diamond substrates.[86] Consequently, the intrinsic thermal conductance per unit area of the F21PA molecule is given by

$$\frac{1}{h_{K,total}} = \frac{1}{h_{K,sapphire}} + \frac{1}{h_{F21PA}} \quad (1)$$

where $h_{K,total}$ is the measured thermal boundary conductance of across metal/PA/sapphire interface, $h_{K,sapphire}$ is the Kapitza conductance across the metal/sapphire interface (without PA molecules), and h_{F21PA} is the intrinsic thermal conductance in the molecule. Figure 6 demonstrates that the calculation of

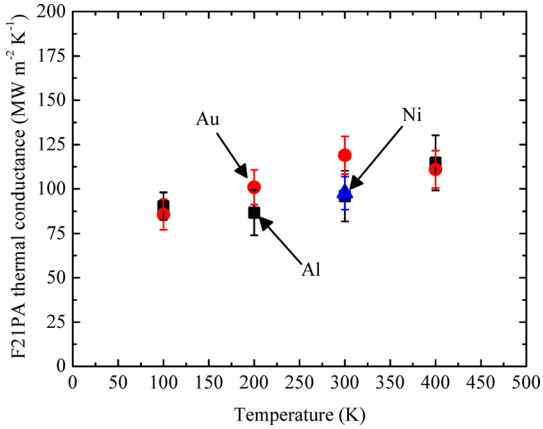

Figure 6. Thermal conductance per unit area of the F21PA molecule as a function of temperature. The consistency in these values, determined from the TDTR measurements on the various metal/F21PA/sapphire samples, indicates that the majority of the thermal scattering across these interfaces is due to diffusive vibrational scattering in the F21PA molecule. The increase in conductance with temperature also indicates that anharmonic scattering of vibrations in the molecule is contributing to thermal conductance.

thermal conductance in F21PA is constant regardless of the choice of metal transducer, further supporting the validity of eq 1 and our assumption that resistance at the metal/F21PA interface is negligible for our samples. The consistency in these values indicates the majority of thermal scattering across these interfaces is due to diffusive vibrational scattering in the F21PA molecule. If the metal films were poorly bonded to the molecule, introducing another relevant resistance to thermal transport in the system, we would expect to see variations in the calculation of F21PA thermal conductance instead of the consistent values we observe regardless of the transducer. As an additional support to diffusive scattering, the increase in conductance with temperature implies that anharmonic scattering of vibrations in the molecule are contributing to thermal conductance. It is interesting to note that the effective

DOI: 10.1021/acs.jpcc.5b05462
J. Phys. Chem. C 2015, 119, 20931−20939

thermal conductivity of F21PA, determined by multiplying the thermal conductance by the molecule length (2 nm) is on the order of 0.2 W m^{-1} K^{-1} at room temperature. This is remarkably similar to a number of common polymers measured in the range of 0.1−0.25 W m^{-1} K^{-1}.[29,87−89] The sheer mass and number of atoms comprising the F21PA molecule, as it becomes large enough to accommodate internal scattering, may account for this similarity between the effective thermal conductivity of the molecule and larger polymer species.

CONCLUSIONS

In summary, we have experimentally studied the thermal transport mechanisms in various phosphonic acid molecules and associated interfaces through thermal conductance measurements across a series of metal/PA/sapphire interfaces. For the three metallic contacts considered in this work (Au, Al, and Ni), we conclude that both the metal/PA and PA/sapphire interfaces do not significantly affect the thermal transport from the metal into the sapphire for the majority of the PAs examined in this study. Furthermore, the temperature trends in thermal conductance measured for the various metal/PA/sapphire boundaries, exclusive of F21PA, suggest that heat transport across these PA contacts is driven by the phononic spectra in the metal and sapphire and not influenced by the vibrational spectra of the PA, in line with previous results from Majumdar et al.[76] For the heaviest molecule, F21PA, we observe a large reduction in thermal conductance across the metal/F21PA/sapphire interface, which we attribute to diffusive scattering in the F21PA molecule and not to interfacial bonding effects. The effective thermal conductivity of this single F21PA molecule is remarkably similar to the thermal conductivity of various polymers, suggesting that the diffusive scattering mechanisms that govern heat transport in disordered polymers may remain the same down to the single molecule level.

EXPERIMENTAL SECTION

Metal/Phosphonic Acid/Sapphire Sample Fabrication. Polished sapphire ⟨0001⟩ wafers, 0.5 mm thick, were purchased from MTI Instruments and diced into 1 cm × 1 cm squares. All substrates were cleaned by a detergent/solvent (DSC) cleaning procedure, consisting of sonication in successive solutions of sodium dodecyl sulfate (SDS) in deionized water followed by sonication in deionized water, and finally ethanol for 10 min each followed by drying in a flow of inert gas. Oxygen (O_2) plasma treatment has been found to clean the substrates of carbon contamination and also significantly increase the amount of phosphonic acid surface coverage by likely increasing the amount of surface hydroxylation.[53,54] Hence, oxygen plasma treatment was performed after DSC cleaning using a Surfx Technologies, He/O_2 atmospheric plasma cleaner operated at 140 W for 5 min followed by immediate reaction with the modifier. The sapphire substrates were modified with the various PAs using a spray modification technique[90] using an Iwata HP-SB Plus airbrush directly after plasma treatment. The substrates were heated to a temperature of 150 °C during the spray modification process to enable rapid bonding of the PA to the substrate and improve surface coverage of the PA. The spray modification technique has the advantage of providing faster surface modification over traditional dip coating methods with monolayer surface coverage. Details of the PA spray coating technique and comparison with dip coating are discussed elsewhere.[90] The concentration of the various PAs used in this study was 10 mM, except in the case of F21PA where the concentration was 5 mM. Post surface modification, the substrates were sonicated for 30 min in a 5% v/v of triethylamine in ethanol to remove any multilayers and physisorbed molecules, leaving behind only covalently bound molecules. Finally, copious rinsing in ethanol is performed to remove any remnants of the triethylamine from the substrate. Further information on the PA characterization is detailed in the Supporting Information.

Time Domain Thermoreflectance Measurements. TDTR is a noncontact optical pump−probe technique, which utilizes short-pulsed lasers to both induce and monitor heating events on the surface of a sample. The output from our 800 nm central wavelength, ∼11 nm bandwidth, 80 MHz repetition rate femtosecond laser is split into a pump path, which is subsequently frequency doubled to 400 nm, and a probe path, in which the optical path length of this probe is adjusted by a mechanical delay stage. This experimental setup affords the ability to monitor the change in thermoreflectivity of the sample with subpicosecond resolution. The pump path is modulated at 8.8 MHz, and an RF lock-in amplifier is used to detect small changes in reflectivity of the probe beam at the modulation frequency of the pump. The ratio between the in-phase and out-of-phase voltage ($-V_{in}/V_{out}$) is monitored via the lock-in amplifier. Established models and analyses are then used to relate the change in reflectivity to the thermal properties metal/PA/sapphire samples.[61,68,69,71] In our measurements, the thermal response at the surface is related to the thermal conductivity and heat capacity of the metal transducer and substrate as well as the thermal boundary conductance across the metal/SAM/sapphire interface. We assume literature values for the heat capacities of each of the metal layers[91] as well as for the heat capacity and thermal conductivity of the sapphire substrate. We are negligibly sensitive to the thermal conductivity of the metal transducers due to the size of our pump and probe spot sizes (average $1/e^2$ radii of ∼12.5 and 6 μm, respectively) and the choice of modulation frequency. We are then left with only the thermal boundary conductance across the metal/PA/sapphire boundary as the most sensitive unknown in our thermal model, which we adjust to determine the thermal boundary conductance across the metal/PA/sapphire interface.

ASSOCIATED CONTENT

Supporting Information

The Supporting Information is available free of charge on the ACS Publications website at DOI: 10.1021/acs.jpcc.5b05462.

Additional characterization of the phosphonic acid molecules, synthesis information for the (3,3,4,4,5,5,-6,6,7,7,8,8,9,9,10,10,11,11,12,12,12-henicosafluorododecyl)phosphonic acid (F21PA) molecules, and TDTR details, sensitivity, and uncertainty analyses (PDF)

AUTHOR INFORMATION

Corresponding Authors

*E-mail phopkins@virginia.edu; Tel +1 434 982-6005; Fax +1 434 982-2047 (P.H.).

*E-mail sgraham@gatech.edu; Tel +1 404 894-2264; Fax +1 404 894-8496 (S.G.).

Notes

The authors declare no competing financial interest.

DOI: 10.1021/acs.jpcc.5b05462
J. Phys. Chem. C 2015, 119, 20931−20939

■ ACKNOWLEDGMENTS

P.E.H. is grateful for support from the Office of Naval Research Young Investigator Program (N00014-13-4-0528). A.J.G. is grateful for support from a NSF graduate research fellowship DGE-0644493.

■ REFERENCES

(1) Ravichandran, J.; Yadav, A. K.; Cheaito, R.; Rossen, P. B.; Soukiassian, A.; Suresha, S.; Duda, J. C.; Foley, B. M.; Lee, C.-H.; Zhu, Y. Crossover from Incoherent to Coherent Phonon Scattering in Epitaxial Oxide Superlattices. *Nat. Mater.* **2014**, *13*, 168−172.

(2) Luckyanova, M. N.; et al. Coherent Phonon Heat Conduction in Superlattices. *Science* **2012**, *338*, 936−939.

(3) Rawat, V.; Koh, Y. K.; Cahill, D. G.; Sands, T. D. Thermal Conductivity of (Zr,W)N/Scn Metal/Semiconductor Multilayers and Superlattices. *J. Appl. Phys.* **2009**, *105*, 024909.

(4) Pernot, G.; et al. Precise Control of Thermal Conductivity at the Nanoscale through Individual Phonon-Scattering Barriers. *Nat. Mater.* **2010**, *9*, 491−495.

(5) Chiritescu, C.; Cahill, D. G.; Nguyen, N.; Johnson, D.; Bodapati, A.; Keblinski, P.; Zschack, P. Ultralow Thermal Conductivity in Disordered, Layered Wse_2 Crystals. *Science* **2007**, *315*, 351−353.

(6) Costescu, R. M.; Cahill, D. G.; Fabreguette, F. H.; Sechrist, Z. A.; George, S. M. Ultra-Low Thermal Conductivity in W/Al_2o_3 Nanolaminates. *Science* **2004**, *303*, 989−990.

(7) Chen, P.; Katcho, N.; Feser, J.; Li, W.; Glaser, M.; Schmidt, O.; Cahill, D. G.; Mingo, N.; Rastelli, A. Role of Surface-Segregation-Driven Intermixing on the Thermal Transport through Planar Si/Ge Superlattices. *Phys. Rev. Lett.* **2013**, *111*, 115901.

(8) Cheaito, R.; Duda, J. C.; Beechem, T. E.; Hattar, K.; Ihlefeld, J. F.; Medlin, D. L.; Rodriguez, M. A.; Campion, M. J.; Piekos, E. S.; Hopkins, P. E. Experimental Investigation of Size Effects on the Thermal Conductivity of Silicon-Germanium Alloy Thin Films. *Phys. Rev. Lett.* **2012**, *109*, 195901.

(9) Swartz, E. T.; Pohl, R. O. Thermal Boundary Resistance. *Rev. Mod. Phys.* **1989**, *61*, 605−668.

(10) Kapitza, P. L. The Study of Heat Transfer in Helium II. *Zh. Eksp. Teor. Fiz.* **1941**, *11*, 1−31.

(11) Hopkins, P. E. Thermal Transport across Solid Interfaces with Nanoscale Imperfections: Effects of Roughness, Disorder, Dislocations, and Bonding on Thermal Boundary Conductance. *ISRN Mech. Eng.* **2013**, *2013*, 682586.

(12) Hopkins, P. E.; Duda, J. C.; Petz, C. W.; Floro, J. A. Controlling Thermal Conductance through Quantum Dot Roughening at Interfaces. *Phys. Rev. B: Condens. Matter Mater. Phys.* **2011**, *84*, 035438.

(13) Duda, J. C.; Hopkins, P. E. Systematically Controlling Kapitza Conductance Via Chemical Etching. *Appl. Phys. Lett.* **2012**, *100*, 111602.

(14) Hopkins, P. E.; Phinney, L. M.; Serrano, J. R.; Beechem, T. E. Effects of Surface Roughness and Oxide Layer on the Thermal Boundary Conductance at Aluminum/Silicon Interfaces. *Phys. Rev. B: Condens. Matter Mater. Phys.* **2010**, *82*, 085307.

(15) Gundrum, B. C.; Cahill, D. G.; Averback, R. S. Thermal Conductance of Metal-Metal Interfaces. *Phys. Rev. B: Condens. Matter Mater. Phys.* **2005**, *72*, 245426.

(16) Hopkins, P. E.; Norris, P. M.; Stevens, R. J.; Beechem, T.; Graham, S. Influence of Interfacial Mixing on Thermal Boundary Conductance across a Chromium/Silicon Interface. *J. Heat Transfer* **2008**, *130*, 062402.

(17) Hopkins, P. E.; Beechem, T. E.; Duda, J. C.; Hattar, K.; Ihlefeld, J. F.; Rodriguez, M. A.; Piekos, E. S. Influence of Anisotropy on Thermal Boundary Conductance at Solid Interfaces. *Phys. Rev. B: Condens. Matter Mater. Phys.* **2011**, *84*, 125408.

(18) Hirotani, J.; Ikuta, T.; Nishiyama, T.; Takahashi, K. Thermal Boundary Resistance between the End of an Individual Carbon Nanotube and a Au Surface. *Nanotechnology* **2011**, *22*, 315702.

(19) Hopkins, P. E.; Adamo, C.; Ye, L.; Huey, B. D.; Lee, S. R.; Schlom, D. G.; Ihlefeld, J. F. Effects of Coherent Ferroelastic Domain Walls on the Thermal Conductivity and Kapitza Conductance in Bismuth Ferrite. *Appl. Phys. Lett.* **2013**, *102*, 121903.

(20) Hopkins, P. E.; Duda, J. C.; Clark, S. P.; Hains, C. P.; Rotter, T. J.; Phinney, L. M.; Balakrishnan, G. Effect of Dislocation Density on Thermal Boundary Conductance across Gasb/Gaas Interfaces. *Appl. Phys. Lett.* **2011**, *98*, 161913.

(21) Gorham, C. S.; et al. Effects of Surface Treatments on Thermal Boundary Conductance Acorss Aluminum/Silicon Interfaces. *Phys. Rev. B: Condens. Matter Mater. Phys.* **2014**, *90*, 024301.

(22) Su, Z.; Huang, L.; Liu, F.; Freedman, J. P.; Porter, L. M.; Davis, R. F.; Malen, J. A. Layer-by-Layer Thermal Conductivities of the Group Iii Nitride Films in Blue/Green Light Emitting Diodes. *Appl. Phys. Lett.* **2012**, *100*, 201106.

(23) Hopkins, P. E.; Baraket, M.; Barnat, E. V.; Beechem, T. E.; Kearney, S. P.; Duda, J. C.; Robinson, J. T.; Walton, S. G. Manipulating Thermal Conductance at Metal-Graphene Contacts Via Chemical Functionalization. *Nano Lett.* **2012**, *12*, 590−595.

(24) O'Brien, P. J.; Shenogin, S.; Liu, J.; Chow, P. K.; Laurencin, D.; Mutin, P. H.; Yamaguchi, M.; Keblinski, P.; Ramanath, G. Bonding-Induced Thermal Conductance Enhancement at Inorganic Heterointerfaces Using Nanomolecular Monolayers. *Nat. Mater.* **2013**, *12*, 118−122.

(25) Losego, M. D.; Grady, M. E.; Sottos, N. R.; Cahill, D. G.; Braun, P. V. Effects of Chemical Bonding on Heat Transport across Interfaces. *Nat. Mater.* **2012**, *11*, 502−506.

(26) Chow, P. K.; Quintero, Y. C.; O'Brien, P.; Mutin, P. H.; Lane, M.; Ramprasad, R.; Ramanath, G. Gold-Titania Interface Toughening and Thermal Conductance Enhancement Using an Organophosphonate Nanolayer. *Appl. Phys. Lett.* **2013**, *102*, 201605.

(27) Hsieh, W.-P.; Lyons, A. S.; Pop, E.; Keblinski, P.; Cahill, D. G. Pressure Tuning of the Thermal Conductance of Weak Interfaces. *Phys. Rev. B: Condens. Matter Mater. Phys.* **2011**, *84*, 184107.

(28) Duda, J. C.; Hopkins, P. E.; Shen, Y.; Gupta, M. C. Exceptionally Low Thermal Conductivities of Films of the Fullerene Derivative Pcbm. *Phys. Rev. Lett.* **2013**, *110*, 015902.

(29) Duda, J. C.; Hopkins, P. E.; Shen, Y.; Gupta, M. C. Thermal Transport in Organic Semiconducting Polymers. *Appl. Phys. Lett.* **2013**, *102*, 251912.

(30) Wang, X.; Liman, C. D.; Treat, N. D.; Chabinyc, M. L.; Cahill, D. G. Ultralow Thermal Conductivity of Fullerene Derivatives. *Phys. Rev. B: Condens. Matter Mater. Phys.* **2013**, *88*, 075310.

(31) Losego, M. D.; Blitz, I. P.; Vaia, R. A.; Cahill, D. G.; Braun, P. V. Ultralow Thermal Conductivity in Organoclay Nanolaminates Synthesized Via Simple Self-Assembly. *Nano Lett.* **2013**, *13*, 2215−2219.

(32) Liu, J.; Yoon, B.; Kuhlmann, E.; Tian, M.; Zhu, J.; George, S. M.; Lee, Y.-C.; Yang, R. Ultralow Thermal Conductivity of Atomic/Molecular Layer-Deposited Hybrid Organic-Inorganic Zincone Thin Films. *Nano Lett.* **2013**, *13*, 5594.

(33) Ong, W.-L.; Rupich, S. M.; Talapin, D. V.; McGaughey, A. J. H.; Malen, J. A. Surface Chemistry Mediates Thermal Transport in Three-Dimensional Nanocrystal Arrays. *Nat. Mater.* **2013**, *12*, 410−415.

(34) Feser, J. P.; Chan, E. M.; Majumdar, A.; Segalman, R. A.; Urban, J. J. Ultralow Thermal Conductivity in Polycrystalline Cdse Thin Films with Controlled Grain Size. *Nano Lett.* **2013**, *13*, 2122−2127.

(35) Wang, R. Y.; Segalman, R. A.; Majumdar, A. Room Temperature Thermal Conductance of Alkanedithiol Self-Assembled Monolayers. *Appl. Phys. Lett.* **2006**, *89*, 173113.

(36) Wang, Z.; Carter, J. A.; Lagutchev, A.; Koh, Y. K.; Seong, N.-H.; Cahill, D. G.; Dlott, D. D. Ultrafast Flash Thermal Conductance of Molecular Chains. *Science* **2007**, *317*, 787−789.

(37) Wang, Z.; Cahill, D. G.; Carter, J. A.; Koh, Y. K.; Lagutchev, A.; Seong, N.-H.; Dlott, D. D. Ultrafast Dynamics of Heat Flow across Molecules. *Chem. Phys.* **2008**, *350*, 31−44.

(38) Segal, D.; Nitzan, A. Heating in Current Carrying Molecular Junctions. *J. Chem. Phys.* **2002**, *117*, 3915−3927.

(39) Segal, D.; Nitzan, A.; Hanggi, P. Thermal Conductance through Molecular Wires. *J. Chem. Phys.* **2003**, *119*, 6840−6855.

DOI: 10.1021/acs.jpcc.5b05462
J. Phys. Chem. C 2015, 119, 20931−20939

(40) Luo, T.; Lloyd, J. R. Non-Equilibrium Molecular Dynamics Study of Thermal Energy Transport in Au–Sam–Au Junctions. *Int. J. Heat Mass Transfer* **2010**, *53*, 1−11.
(41) Luo, T.; Lloyd, J. R. Equilibrium Molecular Dynamics Study of Lattice Thermal Conductivity/Conductance of Au-Sam-Au Junctions. *J. Heat Transfer* **2010**, *132*, 032401.
(42) Zhang, Y.; Barnes, G. L.; Yan, T.; Hase, W. L. Model Non-Equilibrium Molecular Dynamics Simulations of Heat Transfer from a Hot Gold Surface to an Alkylthiolate Self-Assembled Monolayer. *Phys. Chem. Chem. Phys.* **2010**, *12*, 4435−4445.
(43) Duda, J. C.; Saltonstall, C. B.; Norris, P. M.; Hopkins, P. E. Assessment and Prediction of Thermal Transport at Solid–Self-Assembled Monolayer Junctions. *J. Chem. Phys.* **2011**, *134*, 094704.
(44) Polanco, C. A.; Saltonstall, C. B.; Norris, P. M.; Hopkins, P. E.; Ghosh, A. W. Impedance Matching of Atomic Thermal Interfaces Using Primitive Block Decomposition. *Nanoscale Microscale Thermophys. Eng.* **2013**, *17*, 263−279.
(45) Saltonstall, C. B.; Polanco, C. A.; Duda, J. C.; Ghosh, A. W.; Norris, P. M.; Hopkins, P. E. Effect of Interface Adhesion and Impurity Mass on Phonon Transport at Atomic Junctions. *J. Appl. Phys.* **2013**, *113*, 013516.
(46) Tian, Z.; Marconnet, A.; Chen, G. Enhancing Solid-Liquid Interface Thermal Transport Using Self-Assembled Monolayers. *Appl. Phys. Lett.* **2015**, *106*, 211602.
(47) Ge, Z.; Cahill, D. G.; Braun, P. V. Thermal Conductance of Hydrophilic and Hydrophobic Interfaces. *Phys. Rev. Lett.* **2006**, *96*, 186101.
(48) Kikugawa, G.; Ohara, T.; Kawaguchi, T.; Torigoe, E.; Hagiwara, Y.; Matsumoto, Y. A Molecular Dynamics Study on Heat Transfer Characteristics at the Interfaces of Alkanethiolate Self-Assembled Monolayer and Organic Solvent. *J. Chem. Phys.* **2009**, *130*, 074706.
(49) Harikrishna, H.; Ducker, W. A.; Huxtable, S. T. The Influence of Interface Bonding on Thermal Transport through Solid−Liquid Interfaces. *Appl. Phys. Lett.* **2013**, *102*, 251606.
(50) Meier, T.; Menges, F.; Nirmalraj, P.; Holscher, H.; Riel, H.; Gotsmann, B. Length-Dependent Thermal Transport Along Molecule Chains. *Phys. Rev. Lett.* **2014**, *113*, 060801.
(51) Duda, J. C.; English, T. S.; Piekos, E. S.; Soffa, W. A.; Zhigilei, L. V.; Hopkins, P. E. Implications of Cross-Species Interactions on the Temperature Dependence of Kapitza Conductance. *Phys. Rev. B: Condens. Matter Mater. Phys.* **2011**, *84*, 193301.
(52) Hopkins, P. E. Multiple Phonon Processes Contributing to Inelastic Scattering During Thermal Boundary Conductance at Solid Interfaces. *J. Appl. Phys.* **2009**, *106*, 013528.
(53) Paniagua, S. A.; Hotchkiss, P. J.; Jones, S. C.; Marder, S. R.; Mudalige, A.; Marrikar, F. S.; Pemberton, J. E.; Armstrong, N. R. Phosphonic Acid Modification of Indium-Tin Oxide Electrodes: Combined Xps/Ups/Contact Angle Studies. *J. Phys. Chem. C* **2008**, *112*, 7809−7817.
(54) Hotchkiss, P. J.; Jones, S. C.; Paniagua, S. A.; Sharma, A.; Kippelen, B.; Armstrong, N. R.; Marder, S. R. The Modification of Indium Tin Oxide with Phosphonic Acids: Mechanism of Binding, Tuning of Surface Properties, and Potential for Use in Organic Electronic Applications. *Acc. Chem. Res.* **2012**, *45*, 337−346.
(55) Chockalingam, M.; Darwish, N.; Le Saux, G.; Gooding, J. J. Importance of the Indium Tin Oxide Substrate on the Quality of Self-Assembled Monolayers Formed from Organophosphonic Acids. *Langmuir* **2011**, *27*, 2545−2552.
(56) Hanson, E. L.; Schwartz, J.; Nickel, B.; Koch, N.; Danisman, M. F. Bonding Self-Assembled, Compact Organophosphonate Monolayers to the Native Oxide Surface of Silicon. *J. Am. Chem. Soc.* **2003**, *125*, 16074−16080.
(57) Fontes, G. N.; Neves, B. R. A. Effects of Substrate Polarity and Chain Length on Conformational and Thermal Properties of Phosphonic Acid Self-Assembled Bilayers. *Langmuir* **2005**, *21*, 11113−11118.
(58) Knesting, K. M.; Hotchkiss, P. J.; MacLeod, B. A.; Marder, S. R.; Ginger, D. S. Spatially Modulating Interfacial Properties of Transparent Conductive Oxides: Patterning Work Function with Phosphonic Acid Self-Assembled Monolayers. *Adv. Mater.* **2012**, *24*, 642−646.
(59) Hotchkiss, P. J.; Li, H.; Paramonov, P. B.; Paniagua, S. A.; Jones, S. C.; Armstrong, N. R.; Brédas, J. L.; Marder, S. R. Modification of the Surface Properties of Indium Tin Oxide with Benzylphosphonic Acids: A Joint Experimental and Theoretical Study. *Adv. Mater.* **2009**, *21*, 4496−4501.
(60) Koh, S. E.; McDonald, K. D.; Holt, D. H.; Dulcey, C. S.; Chaney, J. A.; Pehrsson, P. E. Phenylphosphonic Acid Functionalization of Indium Tin Oxide: Surface Chemistry and Work Functions. *Langmuir* **2006**, *22*, 6249−6255.
(61) Marcinko, S.; Fadeev, A. Y. Hydrolytic Stability of Organic Monolayers Supported on Tio_2 and Zro_2. *Langmuir* **2004**, *20*, 2270−2273.
(62) Mutin, P. H.; Guerrero, G.; Vioux, A. Hybrid Materials from Organophosphorous Coupling Molecules. *J. Mater. Chem.* **2005**, *15*, 3761−3768.
(63) Donley, C.; Dunphy, D.; Paine, D.; Carter, C.; Nebesny, K.; Lee, P.; Alloway, D.; Armstrong, N. R. Characterization of Indium-Tin Oxide Interfaces Using X-Ray Photoelectron Spectroscopy and Redox Processes of a Chemisorbed Probe Molecule: Effect of Surface Pretreatment Conditions. *Langmuir* **2002**, *18*, 450−457.
(64) Thissen, P.; Valtiner, M.; Grundmeier, G. Stability of Phosphonic Acid Self-Assembled Monolayers on Amorphous and Single-Crystalline Aluminum Oxide Surfaces in Aqueous Solution. *Langmuir* **2010**, *26*, 156−164.
(65) Gao, W.; Dickinson, L.; Grozinger, C.; Morin, F. G.; Reven, L. Self-Assembled Monolayers of Alkylphosphonic Acids on Metal Oxides. *Langmuir* **1996**, *12*, 6429−6435.
(66) Taylor, C. E.; Schwartz, D. K. Octadecanoic Acid Self-Assembled Monolayer Growth at Sapphire Surfaces. *Langmuir* **2003**, *19*, 2665−2672.
(67) Hopkins, P. E.; Serrano, J. R.; Phinney, L. M.; Kearney, S. P.; Grasser, T. W.; Harris, C. T. Criteria for Cross-Plane Dominated Thermal Transport in Multilayer Thin Film Systems During Modulated Laser Heating. *J. Heat Transfer* **2010**, *132*, 081302.
(68) Stoner, R. J.; Maris, H. J. Kapitza Conductance and Heat Flow between Solids at Temperatures from 50 to 300 K. *Phys. Rev. B: Condens. Matter Mater. Phys.* **1993**, *48*, 16373−16387.
(69) Hopkins, P. E.; Salaway, R. N.; Stevens, R. J.; Norris, P. M. Temperature Dependent Thermal Boundary Conductance at Al/Al2o3 and Pt/Al2o3 Interfaces. *Int. J. Thermophys.* **2007**, *28*, 947−957.
(70) Hopkins, P. E.; Stevens, R. J.; Norris, P. M. Influence of Inelastic Scattering at Metal-Dielectric Interfaces. *J. Heat Transfer* **2008**, *130*, 022401.
(71) Hopkins, P. E.; Hattar, K.; Beechem, T.; Ihlefeld, J. F.; Medlin, D. L.; Piekos, E. S. Reduction in Thermal Boundary Conductance Due to Proton Implantation in Silicon and Sapphire. *Appl. Phys. Lett.* **2011**, *98*, 231901.
(72) Hopkins, P. E.; Hattar, K.; Beechem, T.; Ihlefeld, J. F.; Medlin, D. L.; Piekos, E. S. Addendum: Reduction in Thermal Boundary Conductance Due to Proton Implantation in Silicon and Sapphire. *Appl. Phys. Lett.* **2012**, *101*, 099903.
(73) Xu, Y.; Kato, R.; Goto, M. Effect of Microstructure on Au/Sapphire Interfacial Thermal Resistanceu/Sapphire Interfacial Thermal Resistance. *J. Appl. Phys.* **2010**, *108*, 104317.
(74) Cahill, D. G.; Goodson, K. E.; Majumdar, A. Thermometry and Thermal Transport in Micro/Nanoscale Solid-State Devices and Structures. *J. Heat Transfer* **2002**, *124*, 223−241.
(75) Schmidt, A. J.; Chen, X.; Chen, G. Pulse Accumulation, Radial Heat Conduction, and Anisotropic Thermal Conductivity in Pump-Probe Transient Thermoreflectance. *Rev. Sci. Instrum.* **2008**, *79*, 114902.
(76) Majumdar, S.; Sierra-Suarez, J. A.; Schiffres, S. N.; Ong, W.-L.; Higgs, I.; Fred, C.; McGaughey, A. J.; Malen, J. A. Vibrational Mismatch of Metal Leads Controls Thermal Conductance of Self-Assembled Monolayer Junctions. *Nano Lett.* **2015**, *15*, 2985−2991.
(77) Kraft, U.; Zschieschang, U.; Ante, F.; Kalblein, D.; Kamella, C.; Amsharov, K.; Jansen, M.; Kern, K.; Weber, E.; Klauk, H.

DOI: 10.1021/acs.jpcc.5b05462
J. Phys. Chem. C 2015, 119, 20931−20939

Fluoroalkylphosphonic Acid Self-Assembled Monolayer Gate Dielectrics for Threshold-Voltage Control in Low-Voltage Organic Thin-Film Transistors. *J. Mater. Chem.* **2010**, *20*, 6416−6418.
(78) Foley, B. M.; Gorham, C. S.; Duda, J. C.; Cheaito, R.; Szwejkowski, C. J.; Constantin, C.; Kaehr, B.; Hopkins, P. E. Protein Thermal Conductivity Measured in the Solid State Reveals Anharmonic Interactions of Vibrations in a Fractal Structure. *J. Phys. Chem. Lett.* **2014**, *5*, 1077−1082.
(79) Shenogin, S.; Bodapati, A.; Keblinski, P.; McGaughey, A. J. H. Predicting the Thermal Conductivity of Inorganic and Polymeric Glasses: The Role of Anharmonicity. *J. Appl. Phys.* **2009**, *105*, 034906.
(80) Leitner, D. M. Energy Flow in Proteins. *Annu. Rev. Phys. Chem.* **2008**, *59*, 233−259.
(81) Sharma, A.; Kippelen, B.; Hotchkiss, P. J.; Marder, S. R. Stabilization of the Work Function of Indium Tin Oxide Using Organic Surface Modifiers in Organic Light-Emitting Diodes. *Appl. Phys. Lett.* **2008**, *93*, 163308.
(82) Spori, D. M.; Venkataraman, N. V.; Tosatti, S. G.; Durmaz, F.; Spencer, N. D.; Zürcher, S. Influence of Alkyl Chain Length on Phosphate Self-Assembled Monolayers. *Langmuir* **2007**, *23*, 8053−8060.
(83) Cahill, D. G. Analysis of Heat Flow in Layered Structures for Time-Domain Thermoreflectance. *Rev. Sci. Instrum.* **2004**, *75*, 5119−5122.
(84) Kittel, C. *Introduction to Solid State Physics*, 7th ed.; John Wiley and Sons, Inc.: New York, 1996.
(85) Cheaito, R.; et al. Thermal Boundary Conductance Accumulation and Interfacial Phonon Transmission: Measurements and Theory. *Phys. Rev. B: Condens. Matter Mater. Phys.* **2015**, *91*, 035432.
(86) Monachon, C.; Weber, L. Influence of a Nanometric Al_2o_3 Interlayer on the Thermal Conductance of an Al/(Si, Diamond) Interface. *Adv. Eng. Mater.* **2015**, *17*, 68−75.
(87) Ghossoub, M. G.; Lee, J.-H.; Baris, O. T.; Cahill, D. G.; Sinha, S. Percolation of Thermal Conductivity in Amorphous Fluorocarbons. *Phys. Rev. B: Condens. Matter Mater. Phys.* **2010**, *82*, 195441.
(88) Kikuchi, T.; Takahaski, T.; Koyama, K. Temperature and Pressure Dependence of Thermal Conductivity Measurement of Polystyrene and Polycarbonate. *J. Macromol. Sci., Part B: Phys.* **2003**, *42*, 1097−1110.
(89) Losego, M. D.; Moh, L.; Arpin, K. A.; Cahill, D. G.; Braun, P. V. Interfacial Thermal Conductance in Spun-Cast Polymer Films and Polymer Brushes. *Appl. Phys. Lett.* **2010**, *97*, 011908.
(90) Bulusu, A.; Paniagua, S. A.; MacLeod, B. A.; Sigdel, A. K.; Berry, J. J.; Olson, D. C.; Marder, S. R.; Graham, S. Efficient Modification of Metal Oxide Surfaces with Phosphonic Acids by Spray Coating. *Langmuir* **2013**, *29*, 3935−3942.
(91) Touloukian, Y. S.; Buyco, E. H. *Thermophysical Properties of Matter - Specific Heat: Metallic Elements and Alloys*; IFI/Plenum: New York, 1970; Vol. *4*.

DOI: 10.1021/acs.jpcc.5b05462
J. Phys. Chem. C 2015, 119, 20931−20939